# Carbon-11-Methionine PET Imaging of Malignant Melanoma

Paula Lindholm, Sirkku Leskinen, Kjell Någren, Pertti Lehikoinen, Ulla Ruotsalainen, Mika Teräs and Heikki Joensuu

*Department of Oncology and Radiotherapy, Radiopharmaceutical Chemistry Laboratory, Cyclotron/PET Center, University of Turku, Turku, Finland*

The purpose of the study was to assess the feasibility of PET and L-[methyl-$^{11}$C]methionine ($^{11}$C-methionine) in the detection of malignant melanoma. **Methods:** Ten patients diagnosed with malignant melanoma (two with primary melanoma and eight with metastatic melanoma of the skin) but had no liver metastases underwent a PET study before starting cancer therapy. Dynamic scanning was performed for 40 min in seven patients and 10–20 min in three patients 25–45 min postinjection. **Results:** Carbon-11-methionine PET detected all melanoma lesions greater than 1.5 cm (n = 22) in diameter, whereas five smaller pulmonary lesions were not detected. The average standardized uptake value of the untreated lesions was 6.3 ± 2.1 (n = 19) and the uptake rate (influx constant) was 0.085 ± 0.041 $min^{-1}$ (n = 16). **Conclusion:** PET imaging with $^{11}$C-methionine is an effective method for visualizing melanoma. It may also be useful in measuring tumor metabolic activity in vivo.

**Key Words:** positron emission tomography; melanoma; carbon-11-methionine

**J Nucl Med 1995; 36:1806–1810**

The incidence of malignant melanoma is rapidly increasing in many western countries (*1,2*), and its prognosis depends largely on the stage of the disease at presentation (*2*). Surgical excision is curative for early primary melanoma, but there has been no effective treatment for advanced metastatic disease. Some improvement, however, may be obtained by combining biological therapy with cytostatics (*3,4*).

In nuclear medicine, malignant melanoma has been studied with monoclonal antibodies (*5,6*), iodinated radiopharmaceuticals (*7,8*) and lymphokine-activated killer cells (*9*) using planar imaging or SPECT (*10,11*) and recently with [$^{18}$F]fluorodeoxyglucose (FDG) PET (*12,13*). Whole-body FDG-PET imaging appears to be more accurate and cost-effective than conventional imaging when evaluating the extent of metastatic melanoma (*14*).

Several amino acids and their analogs have been suggested for melanoma-specific imaging. Malignant transformation of the melanocyte that produces the pigment melanin gives rise to melanoma. The production of melanin starts by conversion of L-tyrosine to L-dihydroxyphenylalanine (L-DOPA) by tyrosinase. Melanin precursors, such as tyrosine labeled with $^{11}$C (*15*) or its radioiodinated derivates (*16*) and DOPA labeled with $^{18}$F (*17,18*) or $^{11}$C (*15*), have been used for specific imaging of melanogenesis in rodents. Melanoma has been visualized with PET and [$^{11}$C]DOPA or [$^{11}$C]tyrosine in an animal study (*15*). Carbon-11-methionine (*19*) and [$^{11}$C]alpha-aminoisobutyric acids (*20*) that are not specific precursors for melanin synthesis have been investigated for detecting melanoma. Gamma imaging with $^{11}$C-methionine was useful in imaging tumors in rodents despite elevated activity in the liver, spleen and kidneys.

L-[methyl-$^{11}$C]methionine ($^{11}$C-methionine) has been successful as a tracer in metabolic PET imaging of several types of cancer (*21–25*). Methionine is a precursor of S-adenosyl-L-methionine, the principal methyl group donor (*26*). Unbalanced DNA methylation has been found in melanoma cells (*27–29*) that need increased amounts of methionine for cell growth. PET imaging with $^{11}$C-methionine reflects methionine transport from plasma to tissues (*30*). This study assesses the feasibility of $^{11}$C-methionine PET imaging of malignant melanoma.

## METHODS

### Patients

We studied ten patients who had been remitted to our hospital for oncologic treatment. Written informed consent was obtained from all patients and the study protocol was approved by the hospital's Ethical Board.

Two patients with primary melanoma (the nasal cavity and the external ear) and eight patients with metastatic melanoma of the skin to the lungs, the subcutis or lymph nodes had a total of 27 malignant evaluable lesions (Table 1). All patients underwent a PET study before starting cancer therapy except Patient 9 who had ulcerative subcutaneous metastases on the right leg and received four daily fractions of palliative radiotherapy (total dose 16 Gy) to most of his lesions before the PET study. Four subcutaneous metastases were in the field of view, and, since he had an untreated metastasis on the left groin, only the uptake of the untreated lesion was taken in the analysis. Patient 10 had more than 20 pulmonary

Received Sept. 28, 1994; revision accepted Mar. 7, 1995.
For correspondence or reprints contact: Paula Lindholm, MD, Department of Oncology and Radiotherapy, University of Turku, FIN-20520 Turku, Finland.

**TABLE 1**
Patient Characteristics

| Patient no. | Age | Sex | BMI | P/M | Lesion site | Lesion size (cm) | Methods for localization |
|---|---|---|---|---|---|---|---|
| 1 | 69 | F | 21.1 | M | Cervical lymph node | 4 × 5 | US, palpation |
| 2 | 44 | F | 26.7 | M | Subcutis | 6 × 7 | Palpation |
| | | | | M | Lung (n = 2) | 0.5-1 × 0.5-1 | Chest radiograph |
| 3 | 60 | M | 35.7 | P | Nasal cavity | 1.5 × 4 | US, CT, MRI |
| 4 | 77 | M | 26.3 | M | Subcutis | 2 × 2.5 | Palpation |
| 5 | 26 | M | 25.2 | P | External ear | 2 × 3 | US, CT, MRI |
| | | | | M | Cervical lymph nodes (n = 2) | 1-1.2 × 1-1.4 | |
| 6 | 65 | M | 32.8 | M | Lung | 3 × 3.5 | Chest radiograph |
| 7 | 68 | M | 29.4 | M | Axillary node | 4 × 5 | Palpation |
| 8 | 70 | F | 25.0 | M | Inguinal lymph node | 4 × 5 | CT, palpation |
| 9 | 89 | M | 25.3 | M | Subcutis (n = 4)* | 1.5-2 × 1.5-3 | Palpation |
| 10 | 80 | F | 28.4 | M | Lungs (n > 20)† | 0.5-4 × 0.5-5 | Chest radiograph |

*Four subcutaneous metastases in the field of view, one of which was untreated.
†Multiple lung metastases, 11 of which were in the field of view.
BMI = body mass index (kg/m$^2$) (mean 27.6); P/M = primary/metastasis; US = ultrasound; CT = computed tomography; MRI = magnetic resonance imaging.

metastases, 11 of which were in the field of view. No patient had liver metastases on conventional imaging studies.

All patients underwent careful physical examination and were subjected to chest and/or skeletal radiography, abdominal US, cervical US (n = 3) CT (n = 3) and MRI (n = 2). The nutritional state of the patient was measured as the body mass index (BMI, the body weight divided by the square of the length given in meters). The primary diagnosis was confirmed histologically for all patients. The nature of all lymph node and subcutaneous metastases was confirmed histologically after surgical biopsy, except for Patient 9 who had subcutaneous tumors that were confirmed by fine-needle aspiration biopsy. The nature of the lung metastases was confirmed by clinical follow-up and histological diagnosis at autopsy.

## PET

We used a tomograph that simultaneously produces 15 contiguous slices (8 direct and 7 cross-planes) with a slice thickness of 6.7 mm and an transaxial resolution of 6.1 mm FWHM in the center of the field of view. All data were reconstructed in a 256 × 256 image matrix. The final in-plane resolution in reconstructed and Hann-filtered images was 8 mm FWHM.

Carbon-11-methionine was synthesized as described by Långström et al. with slight modifications (*31*). The radiochemical purity (*32*) was 97.4% ± 1.9% (mean ± s.d.). The impurities were $^{11}$C-methionine sulfoxide and D-$^{11}$C-methionine, which were present in about equal amounts.

Prior to imaging, patients fasted for 3–4 hr. The target area was selected to encompass the malignant lesion and the regional lymph nodes. Transmission scanning to correct for attenuation was performed with a removable $^{68}$Ge ring source (total counts 15-30 × $10^6$ per plane). Immediately after the transmission scan, $^{11}$C-methionine (250 ± 80 MBq) was injected as a bolus into an antecubital vein and dynamic scanning was carried out for 40 min (four 30-sec, three 60-sec, five 180-sec and four 300-sec scans). Patients 1, 6 and 9 were scanned for 10–20 min (two to three 300–600-sec scans) 25–45 min postinjection.

Venous blood sampling from the contralateral arm was performed in seven patients to measure the input function. Labeled methionine metabolites were considered by separating the plasma low molecular weight fraction (LMWF) by fast-gel filtration (*33*). The radioactivity concentration of $^{11}$C-methionine initially increases rapidly, becomes constant from 25 to 40 min postinjection and then declines slightly (*34*). In this study, the plasma input curve was obtained from total plasma radioactivity concentration during the first 15 min and subsequently after correction for labeled metabolites. When radioactivity concentration of plasma LMWF taken at 20, 40 and 60 min postinjection is used as the input function, a straight slope reflecting unidirectional transport of $^{11}$C-methionine into tumor tissue is obtained for a 40-min scan time.

Regions of interest (ROIs) were drawn on sites metabolically representing the most active areas in tumorous and normal tissues, so that the relative standard deviation of the measured radioactivity concentration in the ROI was always smaller than 14% in the last frame. Tracer uptake was measured as the standardized uptake value (SUV):

$$\text{SUV} = \frac{\text{Radioactivity concentration in ROI [Bq cm}^{-3}\text{]}}{\text{Injected dose [Bq]/Patient's weight [g]}}.$$

The ROI with the maximum average radioactivity concentration 35–40 min postinjection, corrected for calibration and decay, was chosen for SUV analysis. The tracer uptake rate was calculated as influx constants ($K_i$ values) using Patlak graphical analysis (*35*). The last seven data points representing the time between 11 and 40 min postinjection were used to produce the influx curve.

**TABLE 2**
Uptake of Carbon-11-Methionine in Malignant Melanoma

| Patient no. | P/M | SUV | $K_i$ value ($min^{-1}$) |
|---|---|---|---|
| 1 | M | 7.5 | — |
| 2 | M (before)* | 5.8 | 0.090 |
| | (after)* | 8.2 | 0.176 |
| 3 | P | 8.6 | 0.079 |
| 4 | M | 5.6 | 0.055 |
| 5 | P | 3.9 | 0.069 |
| | M | 3.8 | 0.065 |
| | M | 2.8 | 0.046 |
| 6 | M (before)* | 5.2 | — |
| | (after)* | 5.2 | 0.067 |
| 7 | M | 12.7 | 0.214 |
| 8 | M | 6.9 | 0.125 |
| 9 | M | 7.3† | — |
| 10 | M (n = 8) | 5.0–7.4 (mean 6.2) | 0.052–0.107 (mean 0.077) |
| Total | n = 19 | 6.3 ± 2.1 (mean ± s.d.) | 0.085 ± 0.041 $min^{-1}$ (mean ± s.d) |

*Before and after the first course of therapy.
†Value for an untreated metastasis.
P/M = primary metatasis.

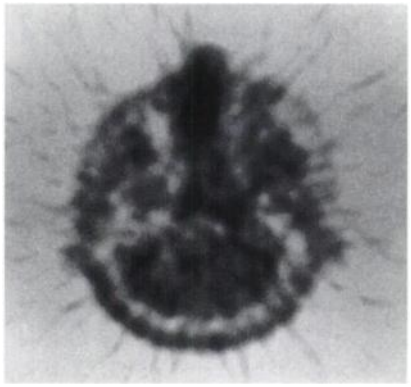

**FIGURE 1.** Primary melanoma of the nasal cavity (Patient 3) is clearly visualized by PET and [$^{11}$C]methionine.

Patients 2 and 6 were studied both before and 4 wk after the first chemotherapy course. Chemotherapy consisted of interferon, dacarbazine, vincristine, bleomycin and lomustine (*3*). There was no change in the size of their metastases at the time of the second PET study. The SUV of a subcutaneous metastasis increased 43%, from 5.8 to 8.2, and the influx constant increased twofold, from 0.090 to 0.176 $min^{-1}$ in Patient 2, who had progressive disease. Carbon-11-methionine uptake in a pulmonary metastasis remained unchanged 1 mo after Patient 6 started chemotherapy. There was partial response only after 7 mo of therapy.

## RESULTS

All 22 malignant lesions larger than 1.5 cm in diameter were visualized (sensitivity 100%), and 22 of 27 lesions of any size were detected with PET and $^{11}$C-methionine (sensitivity 81%). There were no false-positive findings. Five of the 14 pulmonary metastases, all 0.5–1.0 cm in diameter, were not visualized (sensitivity 64%), obviously because of the scanner's resolution limitations, partial volume effects and respiratory movements.

The average SUV in untreated melanoma was 6.3 ± 2.1 (median 6.2; range 2.8–12.7, n = 19) and the influx constant 0.085 ± 0.041 $min^{-1}$ (median, 0.072; range 0.046–0.214, n = 16, Table 2). Linearity of the Patlak curves was excellent ($r^2$ = 0.97–0.99), except in one study (Patient 4, $r^2$ = 0.71). The SUVs of the three irradiated lesions of Patient 9 ranged from 3.3 to 4.1, whereas an untreated metastasis had an SUV of 7.3.

In normal tissues, the highest SUVs were measured in the liver (12.6 ± 3.6, mean ± s.d.; median 12.1; range 7.7–15.4, n = 4). Myocardial SUV varied from 5.8 to 6.8 (n = 2), while the mean uptake in the salivary glands was 5.9 ± 1.3 (median 6.0; range 4.4–6.6, n = 3), and 6.3 ± 1.3 (median 6.0; range 4.6–8.3, n = 9) in the bone marrow.

Image quality was generally good (Fig. 1–3). Metastatic melanoma to the inguinal and iliac nodes was successfully imaged (Patients 8 and 9), and PET image analysis was not impaired despite the close proximity of the tumors to the bladder (Patient 8, Fig. 3B). Tumor detection was impaired in Patient 4, however, who had a subcutaneous metastasis (2 × 2.5 cm) next to the myocardium and in the same axial plane as the liver.

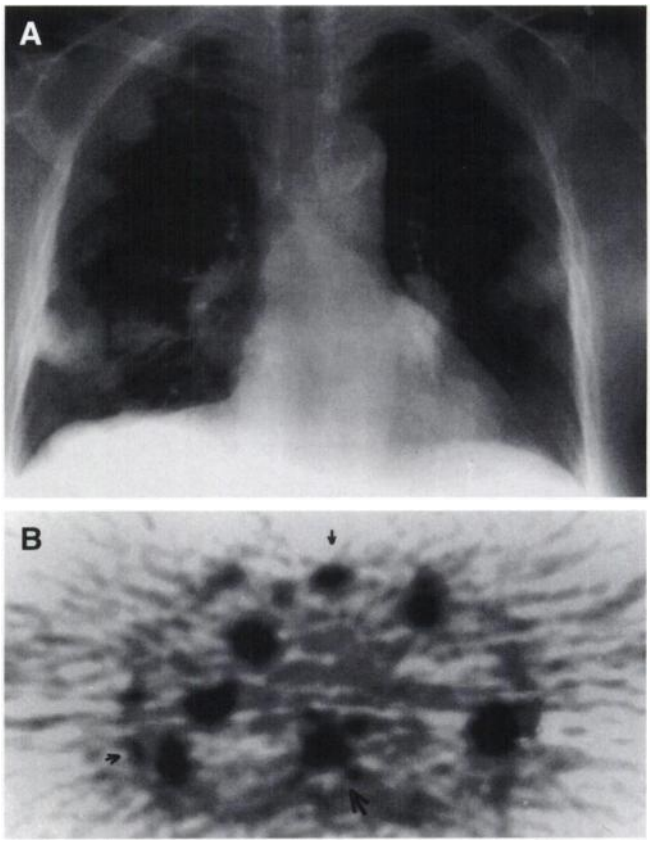


**FIGURES 2.** Malignant melanoma metastatic to the lungs (mean SUV, 6.2; range, 5.0–7.4, Patient 10) was studied by chest radiography (A) and (B) [$^{11}$C]methionine PET. Thoracic vertebra (SUV 8.2), rib cage (SUV 5.2) and sternum (SUV 5.8) are indicated by arrows in the PET scan.

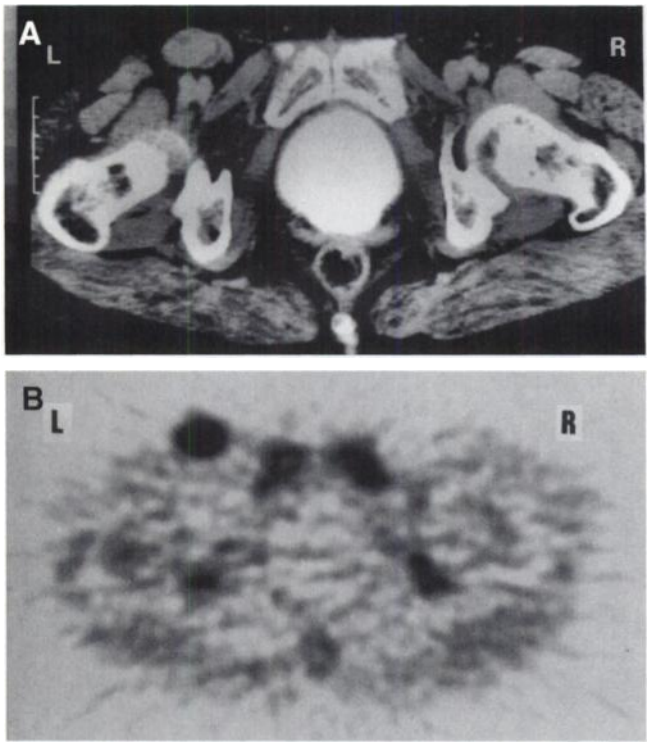


**FIGURES 3.** Metastatic melanoma (Patient 8) to the left inguinal lymph nodes studied by (A) CT and (B) [$^{11}$C]methionine PET. Pubic, iliac and the sacral bones are clearly visible in the PET scan.

## DISCUSSION

In this investigation, the mean SUV in primary and metastatic melanoma varied between 2.8 and 12.7 (6.3 ± 2.1, mean ± s.d.), which corresponds to the mean SUV reported in non-Hodgkin's lymphoma (6.7 ± 2.8) (*23*) but is slightly higher than that found in non-small-cell lung cancer (*36*); it is lower than the mean SUV of breast cancer (8.5 ± 3.3) (*24*) or head and neck cancer (8.5 ± 3.5) (*25*).

Five small (0.5–1.0 cm in diameter) pulmonary metastases were the only malignant lesions not detected by $^{11}$C-methionine PET. Our results agree with those of Gritters et al. (*13*) who found FDG-PET unsuccessful in imaging small (<1.0 cm in size) lung lesions. In their study, average FDG uptake for melanoma lesions >1.5 cm in diameter (7.2 ± 1.2; s.e.) was somewhat higher than the average uptake of $^{11}$C-methionine found in our study.

In animal studies, melanoma has been identified as a heterogenous disease regarding its biological properties and metastatic potential (*37*). We also found that $^{11}$C-methionine uptake in malignant melanoma varied considerably. This should be considered when imaging melanoma metastases in the upper abdominal area.

According to Syrota et al. (*38*), the major problem with using $^{11}$C-methionine PET in this region is the impossibility to differentiate between cancer and pancreatitis. Oikawa et al. (*39*) found FDG to be better than $^{11}$C-methionine in distinguishing pancreatic cancer from benign diseases. Uptake of $^{11}$C-methionine in the liver and the pancreas is high, which impairs detection of metastases with limited tracer uptake in these organs. Because $^{11}$C-methionine accumulates in the bone marrow, its sensitivity in detecting bone metastases needs to be evaluated in further studies.

None of our patients had clinically evident inflammatory or scar tissue in the field of view. In an animal study (*40*), $^{11}$C-methionine uptake in aseptic inflammation was significantly lower than in cancer, but some $^{11}$C-methionine uptake was found in lung granulomas (*41*) and breast (*24*) and brain (*42*) abscesses. Inflammation may also limit the use of FDG (*43,44*) as a tumor-seeking agent. We found $^{11}$C-methionine PET to be useful in distinguishing persistent head and neck cancer from benign irradiation-induced changes (*45*).

Although the incidence of melanoma has been increasing, especially during the past two decades, most new cases are diagnosed at an early stage when it is still curable by surgery. Clinical evaluation of such patients may underestimate the extent of metastatic disease and actual tumor burden (*2*). Accurate staging is of importance, since the number of metastatic nodes is one of the most significant prognostic factors in nondisseminated melanoma (*2*).

Malignant melanoma has been studied with iodinated benzamides and different monoclonal antibodies using planar or SPECT imaging (*7,8,10,11*), but high tracer accumulation in various organs may limit the usefulness of these techniques. Due to its superior contrast resolution and quantitation over conventional nuclear imaging methods, PET scanning with $^{11}$C-methionine may provide a noninvasive tool for detection and regional staging of malignant melanoma in patients who have locally advanced disease, because this method might reveal malignant lesions not detected during clinical examination.

There is some evidence that $^{11}$C-methionine PET could be used to evaluate treatment response in breast (*46*) and lung (*47*) cancer. In one of our patients with clinically progressive melanoma, tracer uptake clearly increased during the first month of therapy but remained constant in another patient who achieved a partial response after several months of therapy. Although these findings are anecdotal, Huovinen et al. (*46*) and Kubota et al. (*47*) found an association between change in $^{11}$C-methionine uptake and treatment response.

## CONCLUSION

PET and $^{11}$C-methionine can be used in metabolic imaging of malignant melanoma. Metastases larger than 1.5 cm in diameter were always visualized. Predicting response to treatment from early changes in $^{11}$C-methionine uptake deserves further study.

## ACKNOWLEDGMENTS

We thank Professors Eeva Nordman and Uno Wegelius for their support and the Nuclear Medicine Department and PET Center personnel for their cooperation. Financial support was provided by the Finnish Cancer Society and the Turku University Foundation.

## REFERENCES


1. Østerlind A. Epidemiology on malignant melanoma in europe. *Acta Oncol* 1992;5:903–908.
2. Balch CM, Houghton AN, Peters LJ. Cutaneous melanoma. In: DeVita VT Jr, Hellman S, Rosenberg SA, eds. *Cancer: principles and practice of oncology*, 4th ed. Philadelphia: Lippincott; 1993:1612–1661.
3. Pyrhönen S, Hahka-Kemppinen M, Muhonen T. A promising interferon plus four-drug chemotherapy regimen for metastatic melanoma. *J Clin Oncol* 1992;10:1919–1926.
4. Legha SS, Buzaid AC. Role of recombinant interleukin-2 in combination with interferon-alfa and chemotherapy in the treatment of advanced melanoma. *Semin Oncol* 1993;20(suppl 9):27–32.
5. Murray JL, Rosenblum MG, Lamki L, et al. Clinical parameters related to optimal tumor localization of indium-111-labeled mouse antimelanoma monoclonal antibody ZME-018. *J Nucl Med* 1987;28:25–33.
6. Eary JF, Schroff RW, Abrams PG, et al. Successful imaging of malignant melanoma with technetium-99m-labeled monoclonal antibodies. *J Nucl Med* 1989;30:25–32.
7. Brandau W, Kirchner B, Bartenstein P, Sciuk J, Kamanabrou D, Schober O. N-(2-diethylaminoethyl)-4-[$^{123}$I]iodobenzamide as a tracer for the detection of malignant melanoma: simple synthesis, improved labeling technique and first clinical results. *Eur J Nucl Med* 1993;20:238–243.
8. Michelot JM, Moreau MF, Veyre AJ, et al. Phase II scintigraphic clinical trial of malignant melanoma and metastases with iodine-123-N-(2-diethylaminoethyl-4-iodobenzamide). *J Nucl Med* 1993;34:1260–1266.
9. Schäfer E, Dummer R, Eilles C, et al. Imaging pattern of radiolabelled lymphokine-activated killer cells in patients with metastatic malignant melanoma. *Eur J Nucl Med* 1991;18:106–110.
10. Wahl RL, Swanson N, Johnson J, et al. Clinical experience with Tc-99m-labeled ($N_2S_2$) anti-melanoma antibody fragments and single-photon emission computed tomography. *Am J Physiol Imaging* 1992;7:48–58.
11. Blend M, Ronan S, Salk D, Gupta T. Role of technetium-99m-labeled monoclonal antibody in the management of melanoma patients. *J Clin Oncol* 1992;10:1330–1337.
12. Lucignani G, Paganelli G, Modorati G, et al. MRI, antibody-guided scintigraphy and glucose metabolism in uveal melanoma. *J Comput Assist Tomogr* 1992;16:77–83.
13. Gritters LS, Francis IR, Zasadny KR, Wahl RL. Initial assessment of positron emission tomography using 2-fluorine-18-fluoro-2-deoxy-D-glucose in the imaging of malignant melanoma. *J Nucl Med* 1993;34:1420–1427.
14. Yao W, Hoh C, Glaspy J, et al. Whole-body FDG-PET imaging for staging of malignant melanoma: is it cost-effective? [Abstract]. *J Nucl Med* 1994; 35(suppl):8P.
15. Van Langevelde A, van der Molen H, Journee-de Korver J, Paans A, Pauwels E, Vaalburg W. Potential radiopharmaceuticals for the detection of ocular melanoma. Part III. A study with $^{14}$C- and $^{11}$C-labeled tyrosine and dihydroxyphenylalanine. *Eur J Nucl Med* 1988;14:382–387.
16. Kloss G, Leven M. Accumulation of radioiodinated tyrosine derivates in the adrenal medulla and in melanomas. *Eur J Nucl Med* 1979;4:179–186.
17. Ishiwata K, Kubota K, Kubota R, Iwata R, Takahashi T, Ido T. Selective 2-[$^{18}$F]fluorodopa uptake for melanogenesis in murine metastatic melanomas. *J Nucl Med* 1991;32:95–101.
18. Kubota R, Yamada S, Ishiwata K, Kubota K, Ido T. Active melanogenesis in non-S phase melanocytes in B16 melanomas in vivo investigated by double-tracer microautoradiography with $^{18}$F-fluorodopa and $^{3}$H-thymidine. *Br J Cancer* 1992;66:614–618.
19. Turner J, Maziere M, Comar D. Localization of $^{11}$C-radiopharmaceuticals in the Greene melanoma of hamsters. *Eur J Nucl Med* 1985;10:392–397.
20. Sordillo PP, DiResta E, Conti PS, et al. Imaging studies using C-11-alpha-aminoisobutyric acid (AIB) in patients with malignant melanoma [Abstract]. *J Nucl Med* 1988;29(suppl):904P.
21. Kubota K, Matsuzawa T, Ito M, et al. Lung tumor imaging by positron emission tomography using C-11-L-methionine. *J Nucl Med* 1985;26:37–42.
22. Ericson K, Lilja A, Bergström M, et al. Positron emission tomography with ([$^{11}$C]methyl)-L-methionine, [$^{11}$C]D-glucose and [$^{68}$Ga]EDTA in supratentorial tumors. *J Comput Assist Tomogr* 1985;9:683–689.
23. Leskinen-Kallio S, Ruotsalainen U, Någren K, Teräs M, Joensuu H. Uptake of carbon-11-methionine and fluorodeoxyglucose in non-Hodgkin's lymphoma: a PET study. *J Nucl Med* 1991;32:1211–1218.
24. Leskinen-Kallio S, Någren K, Lehikoinen P, Ruotsalainen U, Joensuu H. Uptake of $^{11}$C-methionine in breast cancer studied by PET. An association with the size of S-phase fraction. *Br J Cancer* 1991;64:1121–1124.
25. Leskinen-Kallio S, Någren K, Lehikoinen P, Ruotsalainen U, Teräs M, Joensuu H. Carbon-11-methionine and PET is an effective method to image head and neck cancer. *J Nucl Med* 1992;33:691–695.
26. Finkelstein JD, Martin JJ. Methionine metabolism in mammals. *J Biol Chem* 1986;261:1582–1587.
27. Diala ES, Cheah MC, Rowitch D, Hoffman RM. Extent of DNA methylation in human tumor cells. *J Natl Cancer Inst* 1983;71:755–764.
28. Liteplo RG. Altered methionine metabolism in metastatic variants of a human melanoma cell line. *Cancer Lett* 1989;44:23–31.
29. Hoffman RM. Unbalanced transmethylation and the pertubation of the differentiated state leading to cancer. *BioEssays* 1990;12:163–166.
30. Ishiwata K, Kubota K, Murakami M, et al. Re-evaluation of amino acid PET studies: can the protein synthesis rates in brain and tumor tissues be measured in vivo? *J Nucl Med* 1993;34:1936–1943.
31. Långström B, Antoni G, Gullberg P, et al. Synthesis of L- and D-[methyl-$^{11}$C]methionine. *J Nucl Med* 1987;28:1037–1040.
32. Någren K. Quality control aspects in the preparation of [$^{11}$C]-methionine. In: Mazoyer BM, Heiss WD, Comar D, eds. *PET studies on amino acid metabolism and protein synthesis*, 1st ed. Dordrecht: Kluwer; 1993:81–87.
33. Lundqvist H, Stålnacke C-G, Långström B, Jones B. Labeled metabolites in plasma after administration of [$^{11}CH_3$]-L-methionine. In: Greitz T, Widen L, Ingvar D, et al. eds. *The metabolism of the human brain studies with positron emission tomography*. New York: Raven Press; 1985:233–240.
34. Leskinen-Kallio S, Huovinen R, Någren K, et al. Carbon-11-methionine quantitation in cancer PET studies. *J Comput Assist Tomogr* 1992;16:468–474.
35. Patlak CS, Blasberg RG, Fenstermacher JD. Graphical evaluation of blood-to-brain transfer constants from multiple-time uptake data. *J Cereb Blood Flow Metab* 1983;3:1–7.
36. Miyazawa H, Arai T, Iio M, Hara T. PET imaging of non-small-cell lung carcinoma with carbon-11-methionine: relationship between radioactivity uptake and flow-cytometric parameters. *J Nucl Med* 1993;34:1886–1891.
37. Fidler IJ. The biology of human cancer metastasis. *Acta Oncol* 1991;30:669–675.
38. Syrota A, Duquesnoy N, Paraf A, Kellershohn C. The role of positron emission tomography in the detection of pancreatic disease. *Radiology* 1982; 143:249–253.
39. Oikawa H, Takahashi H, Yoshioka T, et al. Differential diagnosis of pancreatic diseases using PET. *CYRIC Annual Report* 1991;274–282.
40. Kubota K, Matsuzawa T, Fujiwara T, et al. Differential diagnosis of AH109A tumor and inflammation by radioscintigraphy with L-[methyl-$^{11}$C]methionine. *Jpn J Cancer Res* 1989;80:778–782.
41. Kubota K, Matsuzawa T, Fujiwara T, et al. Differential diagnosis of lung tumor with positron emission tomography: a prospective study. *J Nucl Med* 1990;31:1927–1933.
42. Ishii K, Ogawa T, Hatazawa J, et al. High L-methyl-[$^{11}$C]methionine uptake in brain abscess: a PET study. *J Comput Assist Tomogr* 1993;17:660–661.
43. Tahara T, Ichiya Y, Kuwabara Y, et al. High [$^{18}$F]-fluorodeoxyglucose uptake in abdominal abscesses: a PET study. *J Comput Assist Tomogr* 1989; 13:829–831.
44. Sasaki M, Ichiya Y, Kuwabara Y, et al. Ring-like uptake of [$^{18}$F]FDG in brain abscess: a PET study. *J Comput Assist Tomogr* 1990;14:486–487.
45. Lindholm P, Leskinen-Kallio S, Grenman R, et al. Evaluation of response to radiotherapy in head and neck cancer with positron emission tomography and [$^{11}$C]methionine. *Int J Radiat Oncol Biol Phys* 1995;32:787–794.
46. Huovinen R, Leskinen-Kallio S, Någren K, Lehikoinen P, Ruotsalainen U, Teräs M. Carbon-11-methionine and PET in evaluation of treatment response of breast cancer. *Br J Cancer* 1993;67:787–791.
47. Kubota K, Yamada S, Ishiwata K, et al. Evaluation of the treatment response of lung cancer with positron emission tomography and L-[methyl-$^{11}$C]methionine: a preliminary study. *Eur J Nucl Med* 1993;20:495–501.